One-dimensional molecular correlations in squaric acid as observed by neutron scattering

K.-D. Ehrhardt and U. Buchenau
Institut für Festkörperforschung, Kernforschungsanlage Jülich, D-5170 Jülich, Germany

E. J. Samuelsen
Fysikkseksjonen, Universitetet i Trondheim, Norges Tekniske Høgskole, N-7034 Trondheim-NTH, Norway

H. D. Maier
Fachrichtung 11.3—Technische Physik, Universität des Saarlandes, D-6600 Saarbrücken, Germany
(Received 16 May 1983)

The nature of the molecular correlation in squaric acid ($H_2C_4O_4$, 3,4-dihydroxy-3-cyclobutene-1,2-dione) was investigated with the use of coherent and incoherent neutron scattering over a wide temperature range. Both types of experiments can be well understood within a model of weakly coupled one-dimensional Ising chains.

I. INTRODUCTION

Since the publication of the structural studies in 1973 by Semmingsen[1] about forty papers have appeared on this unique material. Squaric acid [H_2(SQ)] (3,4-dihydroxy-3-cyclobutene-1,2-dione, $H_2C_4O_4$) is at room temperature a solid consisting of planar squaric C_4O_4 ions linked together by protons in a layered structure (Fig. 1). Each layer is electrically polarized due to proton ordering in the hydrogen bonds between neighboring molecules while the layers are antiferroelectrically stacked along the unique plane normal direction $\vec{b}$. At room temperature H_2(SQ) belongs to the monoclinic space group $P2_1/m$ (C_{2h}^2).[1] A phase transition was discovered at $T_c \simeq 100$ °C to a tetragonal space group $I4/m$ (C_{4h}^5) accompanied by a unit cell halving along $\vec{b}$.[2–4]

The great interest in squaric acid results from its simple structure combined with its interesting properties. Already three lengthy reviews have been written on this single material[5–7] to which we refer for extensive references to various optical, dielectric, ultrasonic, nuclear magnetic resonance, and specific-heat studies, as well as theoretical work. The material was expected to serve as an interesting prototype for testing the role of the dimensionality on the critical behavior, as the early work pointed to an essentially two-dimensional behavior, with an order-parameter index β in the vicinity of the value $\frac{1}{8}$. Subsequent work has thrown some doubt on this point, since there may be a slight discontinuity in the order parameter close to T_c.[6] However, the anisotropy of the diffuse neutron scattering together with other evidence shows that the molecular correlations are indeed anisotropic. As the present work will show, the correlations, in fact, have a pronounced one-dimensional character above T_c. It is fairly clear that the protons play an important role in the phase transition although the strong effect of deuteration on T_c might also be explained by a slight change of geometry.[8] Like for other hydrogen-bonded materials [e.g., KH_2PO_4 (Ref. 9)], several pseudospin models have been used for H_2(SQ) as well as selected vertex models. Deininghaus[10] gives a good survey of this point. It is interesting that Schneider and Tornau[11] and Maier, Müser, and Petersson[12] find on fitting of experimental facts to spin models that the coupling along certain molecular chains comes out particularly strong, indicating a one-dimensional character. In fact ideas along such lines were advanced in informal discussions by various groups.

As will be shown in the present work the neutron scattering data can be well described within the simplest spin model of all, namely that of weakly coupled Ising chains. The dynamics is taken into account by introducing the Glauber model. Our observations of the quasielastic broadening above T_c suggest proton jumps rates of the order of 10^{12} s^{-1} above T_c. It is believed that this effect is due to Ising-type domain-wall movements.

Although most often the Ising pseudospin is identified with the position of the proton in a hydrogen bond, in squaric acid it seems that the proton position is strongly

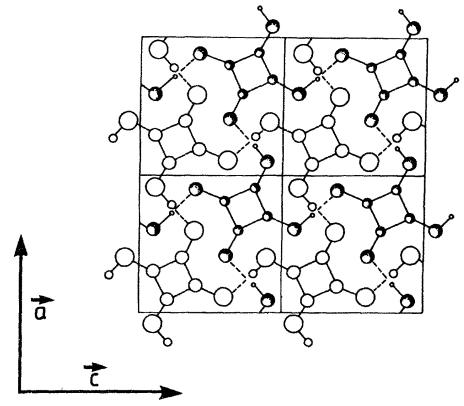

FIG. 1. Structure of squaric acid at room temperature as seen along the monoclinic b axis. Small spheres: hydrogen; intermediate-sized spheres: carbon; large spheres: oxygen. Shaded spheres: at level $y=0$; open spheres: at level $y=\frac{1}{2}$. Lattice constants at 121 °C: $a=6.143$ Å, $b=5.335$ Å, and $c=6.143$ Å.

coupled to the shape of the C_4O_4 molecular frame. Therefore, the pseudospin here should rather be assigned to the whole molecule. The full molecular shape is then to be described by two pseudospins σ_a and σ_c per molecule, associated with the horizontal (a) or the vertical (c) direction.

Some words of comparison should be spent on other hydrogen-bonded materials. KH_2PO_4 already mentioned is truly three dimensional. In this case the proton pseudospin has to be coupled to the lattice motion in order to explain the observed atomic rearrangement at T_c. CsH_2PO_4 (Ref. 13) belonging to the potassium dihydrogen phosphate (KDP) family has a geometry which favors one-dimensional strings of proton ordering, and in fact one dimensionality has been observed above T_c.

Two much studied layer compounds having superficial resemblance to squaric acid are $Cu(HCOO)_2 \cdot 4H_2O$ (CFT) (Ref. 14) and $SnCl_2 \cdot 2H_2O$ (SCD).[15] In both cases the proton system is in layers of H_2O molecules. Unlike CsH_2PO_4 and H_2(SQ), where the O-O distance connected with the H bond is less than 2.55 Å, in the water systems the O-O distance is much larger, about 2.8 Å. Proton ordering is found to behave essentially two dimensionally with T_c in the range of 230 K. Isotope effects are small. For both compounds pronounced two-dimensional correlations are found above T_c (Refs. 14 and 15) and for both cases a dimer model was utilized in the data fitting rather than a pseudospin model. The topology of these two materials differ from that of squaric acid in one essential respect. Whereas in the latter case chains of correlated molecules can cross without affecting each other, this is not possible in the former ones. Consequently CFT and SCD must be truly two dimensional and would not be expected to show correlated strings.

In the present paper we report on a detailed study of squaric acid by means of neutron scattering. Both incoherent (Sec. III) and coherent diffuse studies (Sec. IV) were performed. In Sec. V we give a description of our results in the frame of a coupled Ising-chain model. Short reports on parts of this work have already appeared.[16,17]

II. SAMPLE AND MEASUREMENTS

For protonated samples, it is necessary to use a flat sample geometry in order to avoid multiple scattering. Therefore, several cleaved and oriented crystals of ~ 1 mm thickness covering an area of ~ 2 cm^2 were glued onto a flat aluminum plate. By using the cleavage plane and starting from a crystal with well-defined boundary planes it was possible to keep the orientation of the crystals with respect to each other within 1°. This was tested experimentally by scanning a broad region around the (020) and the (400) reflection in $\vec{Q}$ space with neutrons. In both cases, only one reflection was found with an effective mosaic width of less than 1°.

The aluminum plate with the crystals was mounted into a cryostat. By using liquid nitrogen as a coolant, temperatures down to 90 K were attainable. Without the coolant, temperatures between room temperature and 450 K could be reached. The temperature was regulated and measured using two platinum resistors attached to the sample holder. The sample holder could be rotated around a horizontal axis with a precision of 0.1°.

The neutron scattering measurements were performed on the triple-axis spectrometer SV4 at the reactor DIDO at Jülich. The standard setting with pyrolitic graphite crystals (002 reflection) in the double monochromator and as analyzer and with a wave vector $k_i = 2.665$ Å^{-1} of the incoming neutrons was used. A pyrolitic graphite filter in the incoming beam removed the (004) and (006) monochromator reflections. The collimation sequence was 120′-120′-45′-45′ for the study of the incoherent scattering and 120′-120′-30′-30′ for the investigation of the diffuse coherent scattering in order to get a better resolution in the momentum transfer $\hbar\vec{Q} = \hbar(\vec{k}_i - \vec{k}_f)$ ($\vec{k}_i$ and $\vec{k}_f$ are the wave vector of incoming and scattered neutrons, respectively). The energy resolution in the first case was 0.24 THz and the Q resolution in the second case was of the order of 0.05 Å^{-1}.

III. INCOHERENT SCATTERING STUDY

A. Incoherent scattering

While carbon and oxygen scatter neutrons coherently due to the occurrence of practically only the spinless single isotopes ^{12}C and ^{16}O, hydrogen is a strong incoherent scatterer as well due to nuclear-spin incoherence. Therefore the incoherent neutron scattering in H_2SQ is only due to the protons.

In incoherent scattering, phase factors normally are not present since incoherence derives from self-correlation of the scattering density. However, when the same proton may take two positions (a distance $\vec{d}$ apart), and the jump rate between these sites is large compared with the proton spin-relaxation rate, terms containing $\cos^2[(\vec{Q}\cdot\vec{d})/2]$ and $\sin^2[(\vec{Q}\cdot\vec{d})/2]$ will occur in the scattering function,[18] as is shown in Appendix A. Usually the nuclear spin-relaxation rate is much lower than the characteristic rates observed in neutron scattering (of the order of 10^{12} s^{-1}).

B. Measurements

The incoherent data were taken at a few arbitrary chosen points of the reciprocal space well removed from regions of Bragg scattering or appreciable coherent diffuse scattering. The spectrometer was scanned at constant-Q setting around energy transfer zero, normally in the range -1 to $+1$ THz. Data were taken for two different crystal settings, corresponding to scattering vector $\vec{Q}$ normal to ($Q_\perp$) and almost parallel ($Q_{||}$) to the molecular plane. If the proton motion is confined to the molecular plane, inelasticity should occur only for the latter case, due to the $\sin^2[(\vec{Q}\cdot\vec{d})/2]$ term (see Appendix A), which vanishes for the former case.

In fact as seen from Fig. 2 appreciable inelastic broadening at elevated temperatures is observed only for the $Q_{||}$ case. This is a very important result, because it shows that the proton jumping out of the planes is not significant as compared to in-plane jumping. We believe this

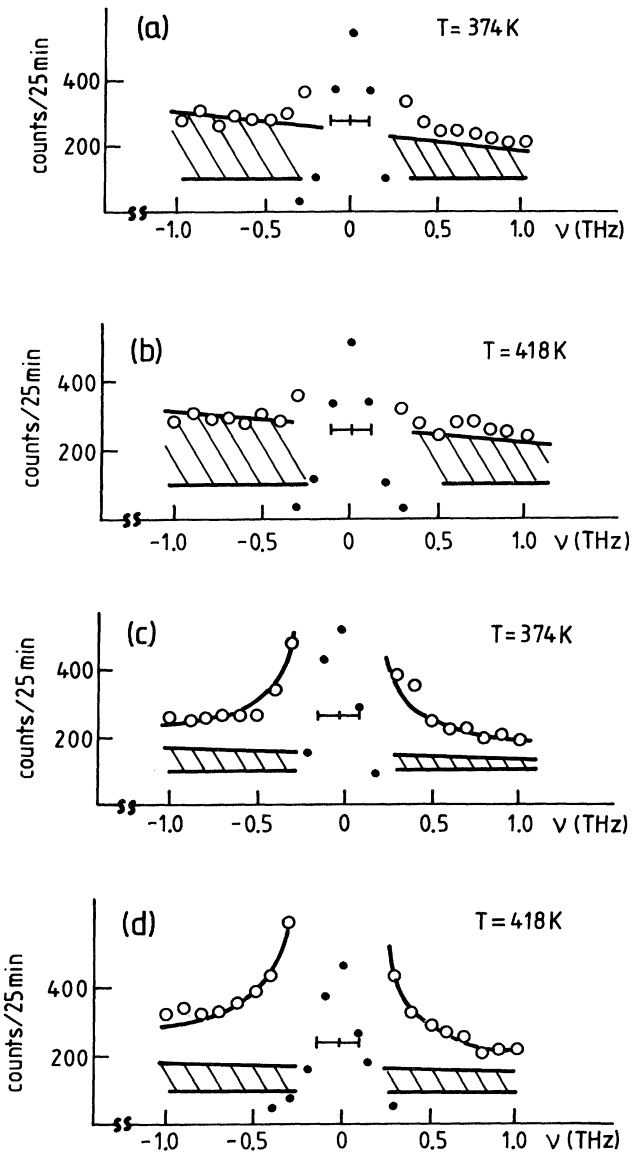

FIG. 2. Incoherent data (a) $Q_\perp$ scan at (0,3.42,0) at 374 K. (b) $Q_\perp$ scan at (0,3.42,0) at 418 K. (c) $Q_{||}$ scan at (3.91, −0.42,0) at 374 K. (d) $Q_{||}$ scan at (3.91, −0.42, 0) at 418 K. Phonon background correction is shown on shaded regions (estimated error 10%, see Sec. III C). ○ represent experiment, the line denotes calculations, ● denotes data (experiment and calculation) which are scaled down by a factor of 10, ⊢⊣ denotes resolution.

is due to a proton motion between two positions of the hydrogen bond.

C. Background correction

The measured intensities had to be corrected for two background contributions: (i) instrumental background and (ii) one-phonon scattering. The instrumental background (i) was measured separately using an empty sample holder. It turned out to be essentially constant independent on energy transfer and temperature. It is shown by the lower continuous line in Fig. 2.

In order to calculate the one-phonon scattering background (ii) it is necessary to make a nontrivial assumption namely that the motion of the proton with the lattice phonons can be considered separately from its jumps between the two sites of the hydrogen bond. In that case one can use the approximation[19]

$$S_{\rm inc}(\vec{Q},\nu)=\int_{-\infty}^{+\infty} d\nu' S^{j}_{\rm inc}(\vec{Q},\nu) S^{\rm osc}_{\rm inc}(\vec{Q},\nu-\nu') ,$$

where $S^{j}_{\rm inc}(Q,\nu)$ is the part of the scattering law due to proton jumps only and $S^{\rm osc}_{\rm inc}(Q,\nu)$ is the part which is due to the phonons. The latter can be treated within a phonon expansion

$$S^{\rm osc}_{\rm inc}(\vec{Q},\nu)=e^{-2w(\vec{Q})}[\delta(\nu)+f_1(\vec{Q},\nu)+\cdots] .$$

In the low-frequency regime, where the slopes of the dispersion curves are still determined by the elastic constants, the phonons are simple acoustic waves with uniform motions of the different atoms in the unit cell. For $h\nu \ll kT$ (ν is the phonon frequency) the quadratic increase in the phonon density of states is compensated by the thermal factor $kT/h\nu$ and a factor $1/\nu$ in the incoherent one-phonon scattering formula.[20] Under these conditions $f_1(\vec{Q},\nu)$ is frequency independent. It can be determined by a suitable average over all phonon wave-vector directions, namely

$$f_1(Q)=\frac{kT}{8\pi^2\rho}\int d\Omega \sum_{n=1}^{3}\frac{(\vec{Q}\cdot\vec{e}_n)^2}{C_n^3} ,$$

Ω denotes the phonon wave-vector direction, $\vec{e}_n$ denotes the polarization vector of the phonon, C_n is the sound velocity (i.e., the slope of the corresponding acoustic branch), and ρ is the density.

We evaluated $f_1(\vec{Q})$ numerically using the elastic constants given by Rehwald and Vonlanthen.[21] The elastic constant C_{13} which had not been measured by the authors was set equal to zero. A variation of C_{13} within reasonable limits ($-10 \le C_{13} \le 10$ GPa) did not change the results by more than 10%. At $T=374$ K and with $Q=4$ Å^{-1}, we get $f_1(\vec{Q})=1.8\times10^{-2}$ THz^{-1} for $\vec{Q}$ in the a-c phase and $f_1(\vec{Q})=5.9\times10^{-2}$ THz^{-1} for $\vec{Q}$ perpendicular to the plane. For our energy resolution [full width at half maximum (FWHM) equal to 0.24 THz] this yields a ratio of 0.46×10^{-2} and 1.5×10^{-2}, respectively, between elastic peak intensity and inelastic one-phonon intensity (at least in a pure phonon picture).

The frequency-independent acoustic-phonon scattering gives rise to a second background term

$$B^{\rm osc}_{\rm inc}(\vec{Q})=F_{\rm norm} f_1(\vec{Q}) .$$

The Debye-Waller factor was omitted in order to take the multiphonon scattering (at least crudely) into account. The normalization factor $F_{\rm norm}$ was determined from the integrated elastic intensity $I_{\rm int}$ at room temperature, where the protons are assumed to move only by taking part in the lattice motion. Then

$$S^{j}_{\text{inc}}(\vec{Q},\nu)=\delta(\nu)$$

and

$$I_{\text{int}}=e^{-2W(Q)}F_{\text{norm}} .$$

Here the oxygen Debye-Waller factor from the structure determination[22] was used in order to stick to the lattice part of the hydrogen motion.

The phonon background calculated in this way is shown as the shaded region in Fig. 2. Note that this contribution is about a factor of 3 larger for the out-of-plane scans, where it accounts for practically the whole observed inelastic intensity. This is in quantitative agreement with the anisotropy of the carbon and oxygen Debye-Waller factors.[22] For the in-plane scans, on the other hand, the correction leaves a distinct quasielastic contribution which increases with increasing temperature and remains visible until well below T_c. In the following this quasielastic contribution will be evaluated in terms of proton jumps between two positions of the hydrogen bond. It should be kept in mind, however, that the validity of the quantitative conclusions depends on the separability of phonon and jumps motions.

D. Results and data fitting

The $Q_{\perp}$ data show a modest peak-height reduction and practically no width variation with increasing temperature. For this case the background variation is fully accounted for by the variation of the phonon contribution.

The $Q_{||}$ data, however, behave differently. Also here the elastic peak height is reduced by increased temperature. In addition a fairly clear broadening is seen near the base of the elastic peak, and furthermore, the wings grow much faster than the estimated phonon background. In fact the peaks may be decomposed into an elastic central peak superimposed on a broader Lorentzian-type contribution, whose typical width is about 1 THz above T_c. In our interpretation this frequency corresponds to the time scale of proton jumps, as discussed in Sec. V C.

As discussed in more detail in Sec. V we found it appropriate to interpret the data in terms of a weakly coupled Ising-chain model, with dynamics included by the Glauber model. The time-dependent self-correlation function $\langle\sigma_j(0)\sigma_j(t)\rangle$ and its Fourier transform, the incoherent scattering function, $G(\nu)$ for this model is given in Appendix C.

This scattering function was folded with the Gaussian instrumental resolution function and then a least-squares fitting to the $Q_{||}$ data was performed at each temperature. The free parameters J_1, α, and C from the fitting to the data are shown in Table I. J_1 is identified with the Ising-chain coupling constant, α is the Glauber jump rate parameter, and C is a parameter taking the neighboring chain coupling into account. As it turns out J_1 and α are somewhat correlated in the fitting. At the final stage J_1 was held fixed at 550 K. As it is seen from Table II, the α values are still not very accurately determined; the two data sets give quite different values. Therefore, only the order of magnitude of α could be determined. The α values for $T<T_c$ are rather unreliable also because of the low level of the inelastic contribution and therefore we do not put any significance to them.

TABLE I. Results of fitting of incoherent data for one set of $Q_{||}$ scans.

T (K)	J_1 (K)	α (THz)	C
294	540	60	1.0
346	600	100	0.6
356	490	50	0.5
374	640	60	0.4
393	590	40	0.23
418	690	90	0.13

IV. DIFFUSE COHERENT SCATTERING

A. Scope of the present work

In their early neutron scattering work Samuelsen and Semmingsen[4] observed a diffuse scattering component existing at several reciprocal-lattice points above T_c. From the detailed study of the distribution of this component around the (4,1,0) reciprocal-lattice point they found that the scattering is extended along the b^* direction, indicating a short molecular correlation range ξ_b in the direction perpendicular to the hydrogen-bonded plane. The scattering is quite sharp in the a^* (c^*) direction, however; therefore the correlation length ξ_a within the planes is large. Owing to resolution limitations a temperature variation of ξ_a was not observed. No attempt was made to interpret the data in any particular model.

The present work brings three new features. Firstly, by improved angular resolution it became possible to identify a temperature variation of ξ_a. Secondly, despite the tetragonal symmetry it turned out to be possible to study the correlation length along chains of squaric acid molecules ξ_a and correlations between chains ξ_c in the same molecular plane. Although the structure is tetragonal a distinction between interchain and intrachain correlation is possible through a favorable weighting of the observations by the scattering structure factor (see Appendix B). Thirdly, a model of a weakly coupled Ising-chain system, having been advanced in informal discussions at various

TABLE II. Results of fitting of incoherent data for two sets of $Q_{||}$ scans with J_1 fixed at 550 K.

Set 1			Set 2		
T (K)	α (THz)	C	T (K)	α (THz)	C
294	120	1.0	294	80	1.0
346	110	0.5	346	60	0.6
			356	100	0.5
373	40	0.5	374	20	0.4
385	90	0.2	393	20	0.23
401	70	0.15			
419	50	0.16	418	20	0.13

occasions, turns out to give an adequate description of both the coherent as well as the incoherent scattering data.

B. Measurements

The same triple-axis instrument was used for both the coherent and the incoherent studies. For the coherent studies the instrument was used in its elastic setting (energy transfer $\nu=0$), and the study was confined to regions around the (4,1,0) reciprocal-lattice point at temperatures above T_c. The sample was oriented with a^*-b^* in the scattering plane. Scans along c^* were performed by tilting the sample.

The instrumental widths Γ_a, Γ_b, and Γ_c along the three directions, were determined experimentally at (4,1,0) below T_c: Γ_a by adding successive scans along h with varying l in the vicinity of $l=0$ and Γ_c by varying the tilt angle of the sample when the spectrometer was centered at (4,1,0). The FWHM is $\Gamma_a=(0.047\pm0.001)a^*$ and $\Gamma_c=(0.062\pm0.004)c^*$.

A rather complete mapping of the diffuse scattering around (4,1,0) was then performed in the a^*-c^* plane at four temperatures: 375 K (102 °C), 381 K (108 °C), 398 K (125 °C), and 416 K (143 °C). The mapping was performed within the limits 3.92—4.08 for h (step-length 0.01) and from -0.4 to 0.4 for l (stepwidth $\sim$0.08), altogether 187 points at each temperature. Supplementary data were taken at 379, 392, and 404 K. Examples of scan data are shown in Fig. 3. Figure 4 shows a contour map around (4,1,0) at 398 K.

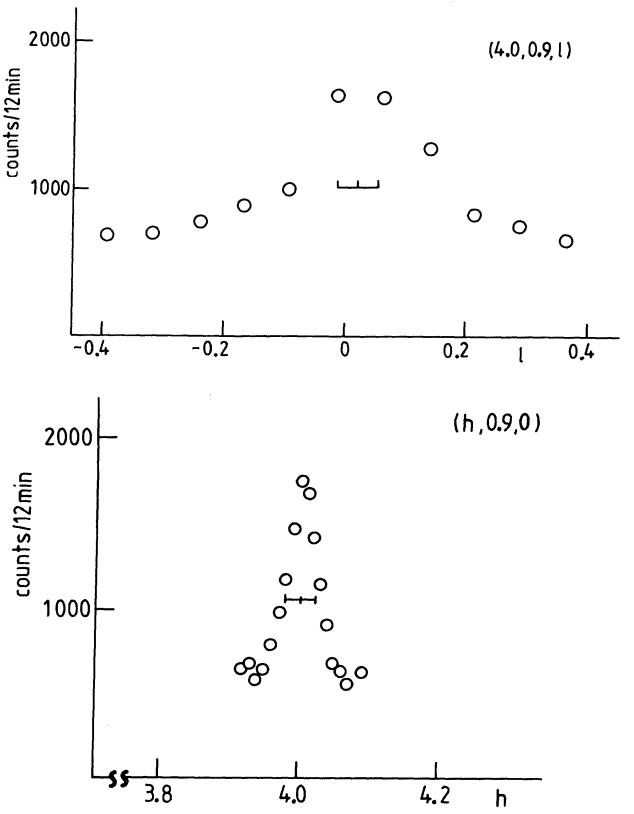

FIG. 3. Example of diffuse scans at 381 K (not corrected for spectrometer setting, background is not subtracted). ⟷ denotes resolution.

C. Results

The diffuse scattering was assumed to be describable by an anisotropic Lorentzian in the form of a wave-vector-dependent susceptibility

$$\chi(\vec{q})=\frac{C}{1+\xi_a^2 q_h^2+\xi_b^2 q_k^2+\xi_c^2 q_l^2}\ , \tag{1}$$

where $\vec{q}=(q_h,q_k,q_l)$ denote the position in the reciprocal space relative to (4,1,0). ξ_a, ξ_b, and ξ_c play the roles of correlation lengths. C is a scale factor.

Equation (1) may be taken as an obvious generalization of the usual three-dimensional isotropic form of $\chi(\vec{q})$. Furthermore, it can be shown to be the exact form for $q \ll a^*,b^*,c^*$ for the model used later. Expressions for ξ_a, ξ_b, and ξ_c in terms of the model are given in Appendix C.

At each temperature a convolution of Eq. (1) with the instrumental resolution was performed in combination with a least-square-fitting procedure to obtain the best values for ξ_a and ξ_c. ξ_b was taken from the data of Ref. 4. Since a two-dimensional numerical convolution in combination with least-squares fitting is very time consuming, a procedure was chosen where first the Lorentzian (1) was fitted in c^* direction to a sum of eight concentric Gaussian functions. Since the instrumental resolution is taken to be Gaussian, an analytic convolution between the instrument and the eight Gaussians could be performed. The remaining convolution in a^* direction was then done by numerical integration.

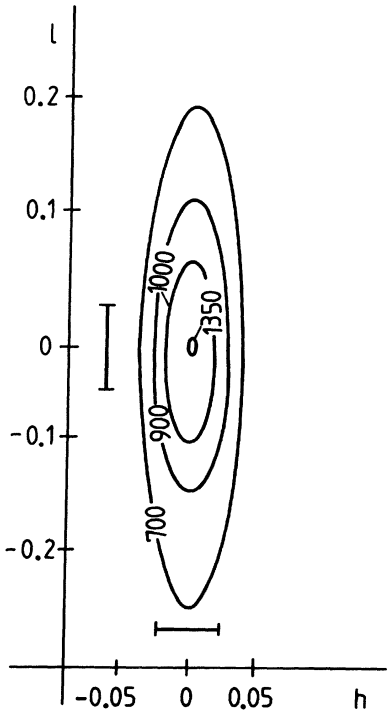

FIG. 4. Contour map in a^*-c^* plane around (4,1,0); ⟷ denotes resolution.

Results of the least-squares fitting are shown in Table III, together with ξ_b data from Ref. 4. The fit to the data at each temperature is generally good, although at 398 K the χ^2 value is somewhat high.

D. Discussion

It is seen that ξ_a is at all temperatures considerably larger than ξ_c and ξ_b, the ratio being roughly $\xi_a:\xi_c:\xi_b=50:5:1$. Thus the tendency towards one-dimensionally correlated chains is quite pronounced. Furthermore, correlations between chains of the same plane are roughly five times stronger than between neighboring planes. It should be remarked that the in-plane correlation is parallel whereas the interplane correlation, although weakest, is antiparallel and of a definite importance, since otherwise the diffuse scattering would not be confined to such reciprocal-lattice points where $h+k+l$ is odd.

Observations at only four temperatures, of course, does not warrant a conclusive analysis of critical indices ν and γ for the temperature variation of the correlation length and the intensity. However, in order to see the trends, we have plotted the values on log-log plots in Figs. 5 and 6. We define as usual

$$\epsilon=(T-T_0)/T_0 , \tag{2}$$

and in case of power-law behavior we expect

$$\xi=\xi_1\epsilon^{-\nu} , \tag{3}$$

and

$$\chi(q=0)=C\epsilon^{-\gamma} . \tag{4}$$

With $T_0=T_c=373$ K we obtain

$$\begin{aligned} &\nu_c=0.33\pm0.07 \quad \text{with } \xi_1^c=5.54 , \\ &\nu_a=0.16\pm0.15 \quad \text{with } \xi_1^a=41.3 , \\ &\nu_b=0.12 \quad \text{with } \xi_1^b=0.67 , \end{aligned} \tag{5}$$

where the value for ν_b is calculated with data from Ref. 4, and

$$\gamma=0.52\pm0.08 . \tag{6}$$

By choosing T_0 lower than T_c all these exponents would increase. For instance $T_0=371$ K gives $\nu_c=0.42\pm0.07$, $\nu_a=0.20\pm0.15$, and $\gamma=0.65\pm0.10$. Values of T_0 lower than 373 K would of course mean that neither the correlation lengths nor the susceptibility $\chi(q=0)$ diverges at the transition temperature. The divergency is quite weak (also for $T_0=T_c$) in accordance with previous findings.[4] In fact the two studies are in agreement in this respect with $\gamma-\nu=0.24\pm0.06$ from Ref. 4 and $\gamma-\nu_a=0.36\pm0.17$ from the present paper. Such critical exponents are not known for any universality class. Deininghaus[23] has proposed that H_2(SQ) rather belongs to a nonuniversal Baxter-model class where exponents depend on interaction strengths. Another possibility is that due to crossover between quasi-one-dimensional behavior and three-dimensional behavior the true critical behavior is only seen in a very narrow temperature region closer to the critical point than was studied here.

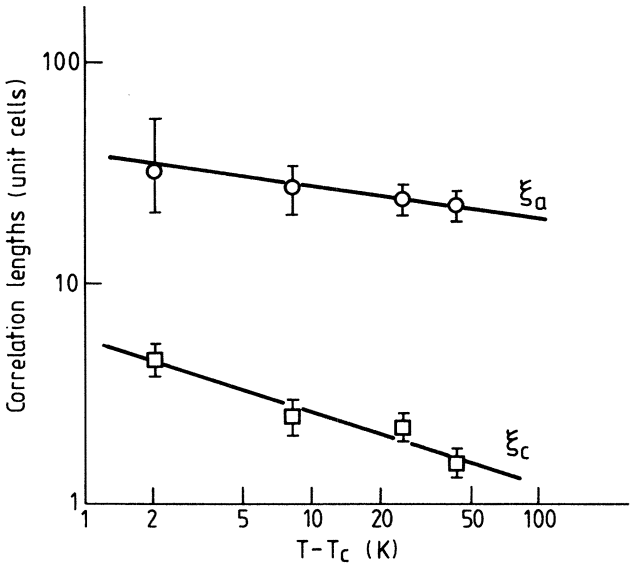

FIG. 5. Correlation length vs $\epsilon=T-T_c$.

V. THE WEAKLY COUPLED ISING-CHAIN MODEL

A. Model

Although the Ising-spin model has its prime application in magnetism, due to its simplicity and easy physical interpretation it is often also applied to order-disorder phenomena in lattice physics. The Ising chain is the simplest model conceivable and it is exactly solvable[24] also in the presence of external fields

$$\mathcal{H}=-J_1\sum_{\substack{\text{chain}\\ i}}\sigma_i\sigma_{i+1}-h\sum_{\substack{\text{chain}\\ i}}\sigma_i , \tag{7}$$

TABLE III. Result of least-squares fitting to the coherent data. ξ_0 and J_1 are values derived from the model. Correlation lengths are given in number of unit cells, J_1 and T in K and scale factor in arbitrary units. ξ_b is taken from Ref. 4.

T (K)	Scale	ξ_a	ξ_c	ξ_b	ξ_0	J_1 (K)
375	274.7	31.6±25	4.4±0.5	0.6±0.1	5.0	431
381	123.5	26.6±3.1	2.3±0.4	0.55±0.1	9.8	512
398	77.5	23.4±3.0	2.2±0.4	0.4±0.1	7.0	525
416	53.8	22.6±3.0	1.5±0.4	0.4±0.1	9.4	610

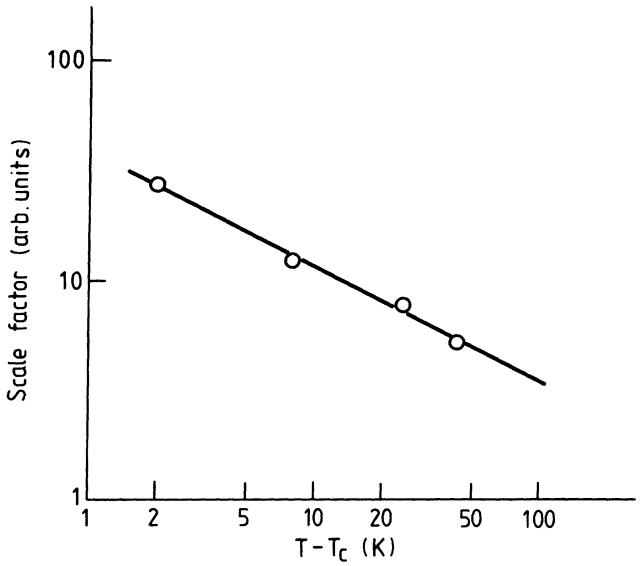

FIG. 6. Scale factor, corresponding to $\chi(q=0)$ vs $\epsilon=T-T_c$.

where the coupling constant J_1 couples nearest neighbors along the chain. The solution is particularly simple for the case of zero field h. For this case the static correlation function is given by[24]

$$\langle \sigma_i \sigma_{i+r} \rangle = \left[\tanh \frac{J_1}{kT} \right]^r , \tag{8}$$

showing that no long-range order appears at finite temperatures for the isolated chain system. In real systems a small interchain coupling will often be present (J_2 for chains within the same plane, J_3 for coupling between planes). Such coupling, although being very weak, will impose on the system a finite long-range-ordering temperature T_c. The interchain coupling is easiest taken into account by mean-field approximation.[25] Results relevant to the present work are given in Appendix C. It should be noticed that the transition temperature depends logarithmically on the ratio J_1/J_2. Furthermore one notices that the generalized susceptibility $\chi(\vec{q})$, has an Ornstein-Zernike form. However, due to the mean-field approximations imposed on the model the critical exponents for the correlation length (ν) and for $q=0$ susceptibility (γ) are predicted to take their mean-field values $\nu_{\mathrm{MF}}=\frac{1}{2}$ and $\gamma_{\mathrm{MF}}=1$. The model predicts that ξ_c should follow a power-law behavior over an extended temperature range, whereas ξ_a would approach the high-temperature limit ξ_0, which is the one-dimensional chain correlation length. ξ_0 should show only a weak temperature dependence of the form $e^{2J_1/kT}$.

The Ising model [Eq. (7)] does not contain any dynamics. A stochastic coupling to the lattice via a heat bath that may induce spin flips, was introduced into the model by Glauber.[26] A pertinent parameter in this model is the quantity α denoting a stochastic spin-flip rate. The time-dependent self-correlation function which is connected to the incoherent neutron scattering function, is given in Appendix C. In squaric acid, we assign to each molecule i two pseudospins, one connected with the horizontal chain direction σ_{ia} and the other connected with the vertical direction σ_{ic} (Fig. 7). We put some attention on the proton position, so that

$$\sigma_{ia} = \begin{cases} +1 \\ -1 , \end{cases}$$

for a right (R) and left (L) proton, respectively, and

$$\sigma_{ic} = \begin{cases} +1 \\ -1 , \end{cases}$$

for an up (U) and down (D) proton, respectively. However, since the whole molecule keeps its low-temperature shape also for $T>T_c$,[4] the various combinations of σ_{ia} and σ_{ic} correspond to the four molecular shapes (orientations) discussed in Appendix B. For coherent neutron scattering it must be assumed that the whole molecule contributes to the scattering. But since only the protons are incoherent scatterers, only their behavior will be reflected through the incoherent scattering observed.

The individual squaric acid molecules carry an electric dipole moment. Its direction and magnitude within the molecular planes could in principle be calculated from linear combination of atomic orbitals (LCAO) treatment of the molecule. Such calculations were recently carried out by Link.[27] It would be a reasonable assumption that the molecular moment is constant, but the direction depends on the actual molecular configurations. Then the dipole moment for an arbitrary molecule is given by

$$\begin{aligned} P_i^x &= A\sigma_{ia} + B\sigma_{ic} , \\ P_i^z &= B\sigma_{ia} + A\sigma_{ic} , \end{aligned} \tag{9a}$$

where

$$A^2 + B^2 = p_0^2 , \tag{9b}$$

and p_0 is the "permanent" molecular dipole moment. From Eq. (9) the total polarization and the dielectric susceptibility can be derived.

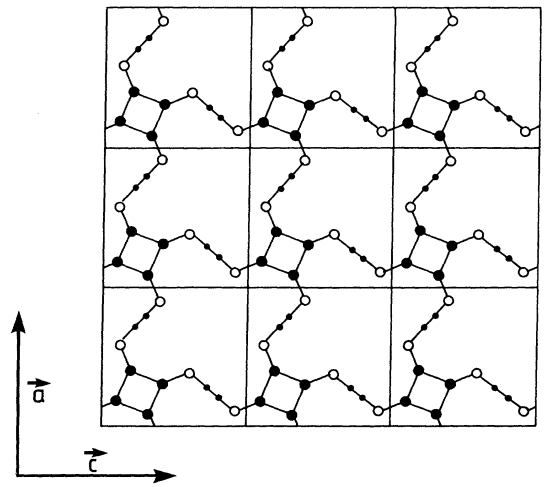

FIG. 7. Single plane of squaric acid.

B. Results of fitting to the model

Both the incoherent and the coherent neutron data could be fitted rather well to the model. In particular a chain coupling constant of about $J_1=550$ K gives a reasonable fit to the two types of data.

For the coherent part the model enters only in the interpretation of the already derived coherence lengths ξ_a, ξ_b, and ξ_c as well as through the value of T_c. From the expressions of Appendix C one can use Eq. (C13) at every temperature to derive the correlation length ξ_0 for a free Ising chain. Since ξ_0 is determined by J_1, a value of J_1 can be derived at each temperature. Although the values show some scatter, an average of $J_1=550\pm50$ K for the three highest temperatures is found, corresponding to $\xi_0\sim8$ unit cells for $T>T_c$.

From the values of ξ_c and ξ_b one can derive J_2 and $|J_3|$, respectively, giving $J_2=0.025J_1$ and $|J_3|=0.0004J_1$. The value of ξ_b is most uncertain. These values would predict a transition temperature $T_c=412$ K. Considering the limitations of the mean-field part of the model the agreement is acceptable.

As already noted the model would predict classical indices ν_c and γ for the temperature dependence of ξ_c and of $\chi(q=0)$. The actual values are considerably lower. In fact one would expect a nonuniversal behavior in the sense that at high temperature a one-dimensional behavior would be seen [$\xi_a\rightarrow\xi_0=\frac{1}{2}\exp(2J_1/kT)$] crossing over first to a two-dimensional behavior in an intermediate range, and finally becoming three-dimensional closer to T_c. The temperature range covered, $\epsilon\lesssim0.12$ is far below the limit $kT_c/2J_1=0.34$ where crossover to higher dimensional behavior would occur.[25] The model would predict ξ_a proportional to ξ_c in the temperature range covered. Since the experimental uncertainties are large for ξ_a at the lowest temperature, it is probably agreement within the experimental uncertainty. As can be seen from Appendix C $\chi(q=0)$ is in fact expected to diverge as $1+2\xi_c^2+2\xi_b^2$. Therefore, $\chi(q=0)$ will diverge with the correlation length which diverges strongest, probably ξ_c and the limiting value for γ is thus

$$\gamma=2\nu_c\ .$$

This is in fact reasonably well observed although the actual values are below the mean-field ones.

C. Dynamics

The Ising model as given by Eq. (7) does not contain any dynamics and is therefore not able to describe frequency-dependent effects. However, dynamics may be put into the model in a statistical sense as shown by Glauber.[26]

In the Glauber model an inverse time α is introduced which is to be identified with the rate of spin flips per spin for a system of independent spins due to stochastic agitation by the surrounding heat bath. Thus α should be proportional to the rate of thermal knocks on the walls of the cage of the pseudospin. It might be tempting to identify α with some vibrational frequency of the system, e.g., with the OH bending or stretching frequency. But it is probably more justified to take α as some average phenomenological constant without a clearcut interpretation. When the spins are not individually free, but are coupled to their neighbors through the Ising coupling constant J_1, they will be less free to jump and the jump rate will be considerably reduced with respect to α.

In Sec. III we already discussed the data fitting to the incoherent scattering. $\alpha=0$ would of course give no energy width, whatever the value of J_1. On the other hand, for $J_1=0$ the peak width would be determined by α alone. Since from the coherent data we observe large one-dimensional correlations along the chains. J_1 must be finite and large. Therefore, since α and J_1 are finite, one has to try and find their optimum values through a data fitting. Not unexpectedly the two parameters are considerably correlated in the fitting procedure, in fact because J_1 enters the model only in products of the type $\alpha\exp(\pm J_1/kT)$. The values of J_1 are found to be in the order of 550 ± 100 K. Although α varies a lot and shows some lack of systematics, it comes out in the range of 50 THz from one set of data and 80 THz from another set, resulting in $\alpha=65\pm25$ THz. This number is of the same order of magnitude as a time constant $\tau_0=2.6\times10^{-14}$ s obtained from ^{13}C NMR data[28] and a characteristic frequency $f_0=30$ THz obtained from dielectric relaxational studies.[29] These frequencies are of the correct order of magnitude to be compared with the OH stretching frequency in squaric acid, which is located to be unusually low, about 1300 cm^{-1} (39 THz).[30,31] On the other hand, it must be admitted that in our case the high flipping rate of an idealized isolated spin may be due to the model. It is possible that the inclusion of a tunneling term in the model would reduce this rate.

The *observed* energy broadening is much lower than this value, being of the order of 1 THz. We believe this frequency to be associated with the average proton jump rate. A correlation length ξ_a would come out as the average length of ordered string pieces of spin either up or down (Fig. 8). The spins at the boundaries are the ones most likely to jump, which would take place at a rate of α corresponding to the (stochastic) motion back and forth of domain boundaries. However, the average rate, experienced by some averages spin will be slower than that by $(2\xi_a)^{-1}$. Since ξ_a is 20–40 units we would get a jump rate of the order of 1–2 THz. As is known moving domain walls in one-dimensional systems can be described as solitons, even for Ising systems.[32]

Specific heat and dielectric properties

With the model at hand one can go on and calculate the above-mentioned properties. In fact such calculations were already performed by Deininghaus.[10] The specific-heat curve obtained by him is shown in Fig. 9. It is noteworthy that there is a huge specific-heat tail above T_c, and the entropy contained under the peak is only a small

FIG. 8. Schematic representation of ordered strings, see text.

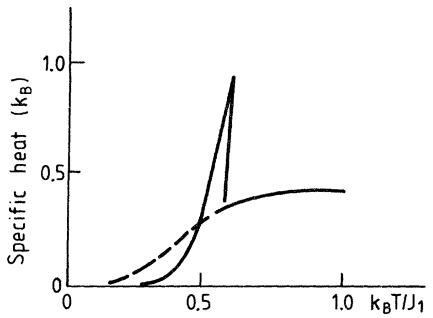

FIG. 9. Specific heat calculated, taken from Ref. 10.

fraction of the total disordering entropy, corroborating the existence of large correlated regions above T_c in agreement with our measurements.

Therefore, in the interpretation of the specific-heat data the background should not be drawn as a smooth line connecting the levels at the two sides of the specific-heat peak. However, it would be difficult to separate the one-dimensional specific-heat tail above T_c from the broad lattice contribution.

The electric polarization and the static dielectric permittivity ξ can easily be calculated. A static measurement corresponds to a zero wavelength study, whereas the diffuse neutron study corresponds to a wavelength $b/2$ along the plane normals (due to the antiferroelectric correlations between neighboring planes). The static susceptibility must have the form of Eq. (C9), only with a sign change in front of J_3 due to the cosine function.

The observed dielectric permittivity is characterized by a very weak temperature dependence of $T > T_c$. It should be noted that the values for ϵ of Refs. 5 and 33 differ by a factor of about 2. We can compose the data with the neutron scattering observations by substituting J_2 and J_3 with the corresponding expressions containing only the correlations lengths, giving

$$\chi_{\text{diel}}=\chi_0\frac{1+2\xi_c^2+2\xi_b^2}{1+4\xi_b^2}\ , \tag{10}$$

where $\chi_0\sim(kT)^{-1}$.

However, with the experimental values from Table III, the fit is still rather poor, although a qualitative improvement is obtained over the mean-field results[10] for the temperature dependence above T_c. The reason for the poor fit is probably because Eq. (10) is not sufficiently general, but relates back to the mean-field treatment of the interchain coupling.

VI. CONCLUSIONS

We have performed incoherent neutron scattering studies over a wide temperature range as well as coherent neutron scattering studies above T_c up to T_c+40 K. Both kinds of experiments are consistent with the existence of pronounced one dimensionality of intermolecular coupling in H_2(SQ). The ratio of correlation lengths $\xi_a:\xi_c:\xi_b$ were found to be of the order of 50:5:1. The temperature variation of the correlation lengths were found to be anomalous, with critical indices ν of the order of only 0.3, and the susceptibility index $\gamma\simeq 0.5$. The indices are rather uncertain, however.

Both kinds of experiments were analyzed using a weakly coupled Ising model, with dynamics of the Glauber model. The intrachain coupling parameter J_1 was determined to 550 K, whereas the in-plane-interchain coupling J_2 is about $0.02J_1$ and the interplanar coupling J_3 is $-0.002J_1$. With these parameters we calculate a transition temperature $T_c=412$ K, in fair agreement with the observed value 373 K. Inelastic broadening of the incoherent scattering corresponds to frequencies of about 1 THz, which is to be associated with the average proton jump rate.

The Glauber rate constant α comes out with a value of about 50 ± 25 THz. This value may probably be associated with the (stochastic) motion back and forth of domain boundaries between oppositely ordered regions of the chains.

ACKNOWLEDGMENTS

The authors thank U. Deininghaus, H. Grimm, J. Petersson, and the co-workers of the Sonderforschungsbereich Ferroelektrika of the Universität des Saarlandes, Saarbrücken for helpful discussions. One of us (E.J.S.) acknowledges financial support from Norges teknisk-naturwitskaplege forskingsråd through the Demines programme for Norwegian—West-German scientific cooperation. He would also like to thank Institut für Festkörperforschung der Kernforschungsanlage Jülich, for hospitality during several stays.

APPENDIX A: INCOHERENT SCATTERING FROM A DOUBLE-WELL PROTON SYSTEM

The incoherent scattering function is determined by the Fourier-transform of the self-correlation function of the scattering density $\rho(\vec{r},t)$ which for a proton system is

$$\rho(\vec{r},t)=\sum_i b_{H_i}\delta(\vec{r}-\vec{R}_i)\ . \tag{A1}$$

The scattering amplitude for the proton will be

$$b_{H_i}=b_{H_{\text{inc}}}e^{-W_H}\left[\frac{[1+\sigma_i(t)]e^{i\vec{Q}\,\vec{d}/2}}{2}+\frac{[1-\sigma_i(t)]e^{-i\vec{Q}\,\vec{d}/2}}{2}\right], \tag{A2}$$

where $\sigma_i(t)$ takes the value $+1$ when the proton is in a right (R) well, say, and -1 when it is in a left (L) well. $\vec{R}_i$ is the vector of the position of the center of the hydrogen bond i. Then the scattering function reads

$$\mathcal{S}(\vec{Q},\nu)=\sum\int\int d^3r\,dt\,e^{i\vec{Q}\cdot\vec{r}}e^{-2\pi i\nu t}\langle\rho_i(0,0)\rho_i(\vec{r},t)\rangle$$
$$=Nb_{H_{\text{inc}}}^2e^{-2W_H}\left[\delta(\nu)\cos^2\left[\frac{\vec{Q}\cdot\vec{d}}{2}\right]+G(\nu)\sin^2\left[\frac{\vec{Q}\cdot\vec{d}}{2}\right]\right], \tag{A3}$$

where

$$G(\nu)=\int dt\langle\sigma_i(0)\sigma_i(t)\rangle e^{-2\pi i\nu t}\,. \tag{A4}$$

The explicit form of $G(\nu)$ for our model is derived in Appendix C.

APPENDIX B: STRUCTURE FACTORS

The diffuse scattering will vary throughout the reciprocal space due to the spatial distribution of the scattering density. In the previous neutron work[4] it was shown that not only the protons but rather the whole molecules give rise to the scattering. Furthermore, the molecules keep their low-temperature shape also above T_c. Therefore, the scattering from the individual molecule in a given reference orientation $F_{\rm mol}(hkl)$ will play an essential role. h, k, and l need not be integers.

Since the present study shows that above T_c the molecules are correlated along chains a distance of several tens of unit cells, whereas the correlation lengths are short in the other two directions, it was found reasonable to estimate structure factors from a model easily manageable: Each molecular string is assumed to possess full order of the protons of the molecules, being to the right (R) or to the left (L) for horizontal strings, up (U) or down (D) for vertical strings. One thus has to do with four types of molecules: RU, LU, RD, LD, the molecular structure factor of which can be calculated:

$$F_{RU}(hkl)=\sum_{\substack{j\\ \text{molecule}}} b_j e^{-W_j}\exp[2\pi i(hx_j+ky_j+lz_j)]\,. \tag{B1}$$

Assuming the same *shape* of the molecules in all orientations, one will see that

$$F_{LU}(hkl)=F_{RU}(lk\bar{h})\,,$$
$$F_{RD}(hkl)=F_{RU}(\bar{l}kh)\,, \tag{B2}$$

and

$$F_{LD}(hkl)=F_{RU}(\bar{h}k\bar{l})\,.$$

The direction of the orientation of the molecule at position (n_a,n_b,n_c) is given by $\sigma_a(n_a,n_b,n_c)=\pm1$ and $\sigma_c(n_a,n_b,n_c)=\pm1$, where the indices a and c are for the horizontal and vertical directions. In our model apparently σ_a is independent of n_a and σ_c is independent of n_c.

With this picture one can develop expressions for the structure factor squared $|F_{\rm tot}|^2$, expressed by the molecular structure factors and σ_a,σ_c. In the final stage independent strings were asumed by imposing the average values

$$\langle\sigma_a\rangle=\langle\sigma_c\rangle=\langle\sigma_a\sigma_c\rangle=0 \tag{B3a}$$

and

$$\langle\sigma_a(n_b,n_c)\sigma_a(n_b',n_c')\rangle=\begin{cases}1 & \text{for } n_b=n_b'\,\Lambda\, n_c=n_c'\\ 0, & \text{otherwise}\,,\end{cases} \tag{B3b}$$

and similarly

$$\langle\sigma_c(n_a,n_b)\sigma_c(n_a',n_b')\rangle=\begin{cases}1 & \text{for } n_b=n_b'\,\Lambda\, n_a=n_a'\\ 0, & \text{otherwise}\,.\end{cases} \tag{B3c}$$

It is convenient to introduce expressions

$$A_R^+=F_{RU}+F_{RD}\,,$$
$$A_R^-=F_{RU}-F_{RD}\,,$$
$$A_L^+=F_{LU}+F_{LD}\,, \tag{B4}$$
$$A_L^-=F_{LU}-F_{LD}\,.$$

Then for the case of ordered chains completely uncorrelated among themselves one finds that $|F_{\rm tot}|^2$ consists of four terms:

$$I_1=|A_R^++A_L^-|^2\delta(Q_a-\tau_a)\delta(Q_b-\tau_b)\delta(Q_c-\tau_c)\,, \tag{B5}$$

which represents fundamental reflections with $h+k+l$ even, sharp in all three directions, existing at all temperatures,

$$I_2=|A_R^-+A_L^-|^2\delta(Q_c-\tau_c)\,, \tag{B6}$$

which represent reflections diffuse in h, sharp in l,

$$I_3=|A_R^+-A_L^+|^2\delta(Q_a-\tau_a)\,, \tag{B7}$$

which represent reflections diffuse in l, sharp in h,

$$I_4=|A_R^--A_L^-|^2\,, \tag{B8}$$

which represent reflections diffuse in both h and l. It should be noticed that the interplanar (anti-correlation) is not taken into account, and that the k dependence of the diffuse components are not included.

From the observed molecular coordinates at room temperature and using the fitted Debye-Waller exponents at 121°C,[22] the structure factors around (4,1,0) are shown in Fig. 10. As is seen the infinite chains along the $\vec{a}$ direction contribute much more to the scattering at (4,1,0) than do the chains along the $\vec{c}$ direction. By this fortunate situation one sees at (4,1,0) in practice only the a chains. [Similarly the c chains would be seen at (0,1,4).]

When the chains are not infinitely long, a width in the h direction will develop from which the correlation length ξ_a can be determined. For obtaining the correlation ξ_c, the slow variation of the diffuse structure factor squared

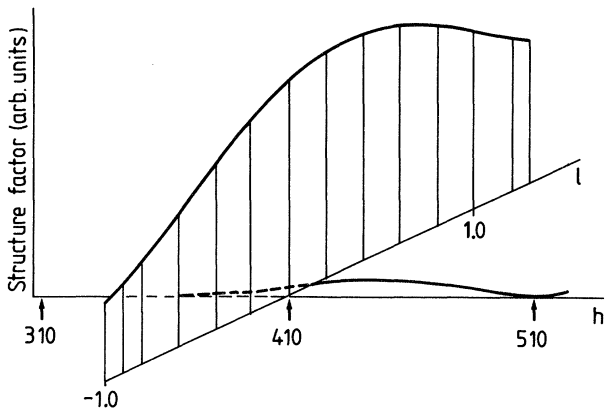

FIG. 10. Structure factor variation around (4,1,0).

is unimportant since the observed width is of the order of $0.2c^*$.

APPENDIX C: THE WEAKLY COUPLED ISING MODEL

The time-dependent spin-correlation function for a one-dimensional Ising chain was already given by Glauber:[26]

$$\langle\sigma_j(0)\sigma_k(t)\rangle=\exp(-\alpha\,|\,t\,|\,)\sum_{l=-\infty}^{\infty}\eta^{|j-k+l|}I_l(\alpha\gamma\,|\,t\,|\,)\,, \tag{C1}$$

with the definitions: $\eta=\tanh(\beta J_1)$, $\gamma=\tanh(2\beta J_1)$, I_n is the modified Bessel function ($I_{-n}\equiv I_n$ for n integer) α is the inverse characteristic time in the Glauber model, β is the inverse temperature. The incoherent neutron scattering function $G(\nu)$ is defined as the Fourier transform of $\langle\sigma_j(0)\sigma_j(t)\rangle$:

$$G(\nu)=2\sum_{l=-\infty}^{+\infty}\eta^{|l|}\int_0^{\infty}e^{-(\alpha+2\pi i\nu)t}I_l(\alpha\gamma t)dt\,. \tag{C2}$$

Using the formula for the Laplace transform of I_δ

$$\mathcal{L}[I_\delta(at)]_{\mathrm{Re}\delta>-1}=a^\delta(p^2-a^2)^{-1/2}\left[\frac{1}{p+(p^2-a^2)^{1/2}}\right], \tag{C3}$$

with $p=\alpha+2\pi i\nu$ and $\mathrm{Re}p>|\,\mathrm{Re}a\,|$ one finds easily

$$G(\nu)=2\,\mathrm{Re}\frac{1}{(p^2-\alpha^2\gamma^2)^{1/2}}\,\frac{p+(p^2-\alpha^2\gamma^2)^{1/2}+\alpha\gamma\eta}{p+(p^2-\alpha^2\gamma^2)^{1/2}-\alpha\gamma\eta}\,, \tag{C4}$$

(C4) gives in the limit $J_1=0$ a Lorentzian as it is used in our preliminary work.[16,17] Formula (1) of Refs. 16 and 17 contains a slight typographical error and should read (using the notation of Ref. 16)

$$I(\omega)\sim e^{-2W(\vec{Q})}\times\left[\delta(\omega)[1-2\omega_1\omega_2\cos(\vec{Q}\cdot\vec{d})]+2\omega_1\omega_2[1-\cos(\vec{Q}\cdot\vec{d})]\frac{\gamma/\pi}{\omega^2+\gamma^2}\right]. \tag{C5}$$

The "hopping" model used in Refs. 16 and 17 which is also related to problems in diffusion theory[34] can be looked upon as a special case ($J=0$) of the model described in the present work.

The dynamics of an Ising chain in the presence of an external field was studied by several authors with application to the helix-coil transition in biopolymers.[35–37] In the paper by Tanaka *et al.*[37] an approximation for the Fourier-transformed autocorrelation function is given. Since Tanaka's expression for $G(\nu)$ contains an integral which only can be solved numerically and $G(\nu)$ itself must be convoluted numerically with the experimental resolution, it does not seem possible to use it for the data fitting because this procedure would be very computer time consuming. Therefore, we suggest for our case of very weak coupling fields a much simpler approximation involving a phenomenological parameter C which accounts for the influence of the coupling field. C is thus a parameter to be fitted,

$$G(\nu)=C\delta(\nu)+2\,\mathrm{Re}\frac{1}{(p^2-\alpha^2\gamma^2)^{1/2}}\times\left[\frac{p+(p^2-\alpha^2\gamma^2)^{1/2}+\alpha\gamma\eta}{p+(p^2-\alpha^2\gamma^2)^{1/2}-\alpha\gamma\eta}-C\frac{p+(p^2-\alpha^2\gamma^2)^{1/2}+\alpha\gamma}{p+(p^2-\alpha^2\gamma^2)-\alpha\gamma^{1/2}}\right], \tag{C6}$$

C varies between zero and one; it should be remarked that the sum rule for the incoherent neutron scattering function

$$\int_{-\infty}^{+\infty}G(\nu)d\nu=1\,, \tag{C7}$$

is fulfilled in our approximation for all values of C. As expected the value of C tends towards zero with increasing temperature (see Tables I and II), but it remains significantly larger than zero above T_c. This may indicate a local order above T_c (Ref. 17) or can be understood as the influence of a random field[38] generated by the neighboring spins.

In the case of vanishing field, the formula given in Ref. 37 can easily be transformed to (C6) using

$$\exp(z\cos\theta)=I_0(z)+Z\sum_{k=1}^{\infty}I_K(z)\cos(k\theta)\,. \tag{C8}$$

Expressions for the generalized susceptibility for the kinetic Ising model with vanishing or small external fields are given by Suzuki and Kubo[39] and by Zumer,[40] respectively. The relations between the generalized susceptibility and the correlation length in a weakly coupled Ising chain were discussed by Scalapino *et al.*[25]

Taking the coupling constant J_1 along the chain, J_2 perpendicular to the chain (intraplanar), and $-J_3$ perpendicular to the chain (interplanar), the susceptibility per spin can be written as

$$\chi(q_1,q_2,q_3)=\frac{\chi_{1d}(q_1)}{1-(2J_2\cos q_2-8J_3\cos q_3)\chi_{1d}(q_1)}\,, \tag{C9}$$

with χ_{1d} as the susceptibility of a one-dimensional system which can be approximated[25] as

$$\chi_{1d}(q_1)=\frac{\chi_0}{1+\xi_0^2q_1^2}\,. \tag{C10}$$

$-J_3$ is used instead of J_3 in order to indicate the antiferroelectric character of this coupling. The components of $\vec{q}$ are taken along the a^*, c^*, and b^* direction, q_1 is defined as a fraction of $a^*=2\pi/a$, q_2, and q_3 similarly. The correlation lengths are therefore directly given in units of cell constants. The factors 2 and 8 in the denominator are the numbers of nearest neighbors. For the analysis of the coherent neutron scattering data the cosine functions in the denominator are expanded around $q_1=0$, $q_2=0$, and $q_3'=q_3-\pi$. One then can express the susceptibility in a form

$$\chi(q_1,q_2,q_3)=\frac{\chi_0}{1+(\xi_a q_1)^2+(\xi_b q_3')^2+(\xi_c q_2)^2}\ , \quad \text{(C11)}$$

where the correlation lengths are given by

$$\xi_a=\frac{\xi_0}{[1-(2J_2+8J_3)\chi_0]^{1/2}}\ ,$$
$$\xi_b=\left[\frac{4J_3\chi_0}{1-(2J_2+8J_3)\chi_0}\right]^{1/2}\ , \quad \text{(C12)}$$
$$\xi_c=\left[\frac{J_2\chi_0}{1-(2J_2+8J_3)\chi_0}\right]^{1/2}\ ,$$

and

$$\xi_a=\xi_0[1+2(\xi_c^2+\xi_b^2)]^{1/2}\ . \quad \text{(C13)}$$

The free-chain correlation length ξ_0 is given by

$$\xi_0=-\ln\{[\tanh(\beta J_1)]^{-1}\}\ . \quad \text{(C14)}$$

As is seen J_1 can be obtained from ξ_0.

[1]D. Semmingsen, Acta Chem. Scand. 27, 3961 (1973).
[2]D. Semmingsen and J. Feder, Solid State Commun. 15, 1369 (1974).
[3]E. J. Samuelsen and D. Semmingsen, Solid State Commun. 17, 217 (1975).
[4]E. J. Samuelsen and D. Semmingsen, J. Phys. Chem. Solids 38, 1275 (1977).
[5]J. Feder, Ferroelectrics 12, 71 (1976).
[6]J. Petersson, Ferroelectrics 35, 57 (1981).
[7]J. Feder, in *Oxocarbons,* edited by R. West (Academic, New York, 1980).
[8]G. A. Samara and D. Semmingsen, J. Chem. Phys. 71, 1401 (1979).
[9]See, for instance, E. M. Lieb and F. Y. Wu, in *Phase Transition and Critical Phenomena,* edited by C. Domb and M. S. Green (Academic, New York, 1972), Vol. 1, p. 332.
[10]U. Deininghaus, Ph.D. thesis, University of Dortmund, Germany, 1982.
[11]V. E. Schneider, and E. E. Tornau, Phys. Status Solidi B 107, 491 (1981).
[12]H. D. Maier, H. E. Müser, and J. Petersson, Z. Phys. B 46, 251 (1982).
[13]B. C. Frazer, O. Semmingsen, W. D. Ellenson, and G. Shirane, Phys. Rev. B 20, 2745 (1979).
[14]R. Youngblood and J. D. Axe, Phys. Rev. B 17, 3639 (1978).
[15]R. Youngblood and J. K. Kjems, Phys. Rev. B 20, 3792 (1979).
[16]U. Buchenau, K. D. Ehrhardt, H. D. Maier, and E. J. Samuelsen, Ferroelectrics 39, 1025 (1981).
[17]E. J. Samuelsen, U. Buchenau, H. D. Maier, K. D. Ehrhardt, E. Fjaer, and H. Grimm, Phys. Scr. 25, 685 (1982).
[18]H. Grimm, H. H. Stiller, and T. Plesser, Phys. Status Solidi 42, 207 (1970).
[19]T. Springer, *Quasielastic Neutron Scattering,* Vol. 64 of *Springer Tracts in Modern Physics* (Springer, Berlin, 1972), p. 34ff, and references therein.
[20]W. Marshall and S. W. Lovesey, *Theory of Thermal Neutron Scattering* (Oxford University Press, Oxford, 1971), p. 89, formula (4.89).
[21]W. Rehwald and A. Vonlanthen, Phys. Status. Solidi B 90, 61 (1978). The agreement with the slopes of the dispersion curves is good as seen in neutron work by E. J. Samuelsen (unpublished).
[22]F. J. Hollander, D. Semmingsen, and T. F. Koetzle, J. Chem. Phys. 67, 4825 (1977).
[23]U. Deininghaus, Z. Phys. B 45, 177 (1981).
[24]C. J. Thompson, *Mathematical Statistical Mechanics* (Princeton University Press, New York, 1972).
[25]D. J. Scalapino, Y. Imry, and P. Pincus, Phys. Rev. B 11, 2042 (1975).
[26]R. J. Glauber, J. Math. Phys. 4, 294 (1963).
[27]K. H. Link (unpublished).
[28]D. Suwelack and M. Mehring, Solid State Commun. 33, 207 (1980).
[29]H. E. Müser, G. Luther, J. Petersson, and R. Kuntz, Phys. Status Solidi A 61, 75 (1980).
[30]S. Nakashima and M. Balkanski, Solid State Commun. 19, 1225 (1976).
[31]D. Bougeard and A. Novak, Solid State Commun. 27, 453 (1978).
[32]L. J. de Jongh, in Proceedings of the International Conference on Magnetism, Montreal, 1982 [J. Magn. Magn. Mater. (to be published)].
[33]H.-D. Maier, D. Müller, and J. Petersson, Phys. Status Solidi B 89, 587 (1981).
[34]K. W. Kehr, R. Kutner, and K. Binder, Phys. Rev. B 23, 4931 (1981).
[35]A. Baumgärtner and K. Binder, J. Stat. Phys. 18, 423 (1978).
[36]A. Baumgärtner and K. Binder, J. Chem. Phys. 70, 429 (1979).
[37]T. Tanaka, A. Wada, and M. Suzuki, J. Chem. Phys. 59, 3799 (1973).
[38]I. Morgenstern, K. Binder, and A. Baumgärtner, J. Chem. Phys 69, 253 (1978).
[39]M. Suzuki and R. Kubo, J. Phys. Soc. Jpn. 24, 51 (1968).
[40]S. Zumer, Phys. Rev. B 21, 1298 (1980).